AIAC14 Fourteenth Australian International Aerospace Congress

Improved simulations of faults in gearboxes for diagnostic and prognostic purposes using a reduced finite element model of the casing

Nader Sawalhi, Lav Deshpande and Robert B. Randall
School of Mechanical and Manufacturing Engineering, University of New South Wales, Sydney 2052, Australia

Abstract

Component mode synthesis (CMS) is an effective technique to reduce the size of large finite element models while keeping the components/modes of interest to achieve an accurate solution in a very efficient manner. In the Craig–Bampton CMS technique, the reduced model is represented as a combination of a number of physical degrees of freedom, the so-called master degrees of freedom and modal degrees of freedom (modal coordinates) which represent the modes of interest in the model. In this paper, the Craig-Bampton CMS method has been employed effectively to couple the model of the casing of a gearbox with a lumped parameter model (LPM) of the internals (shafts, gears, bearings). The latter has the capacity to simulate faults in the gears and bearings. The results show a clear improvement in both the frequency spectra at the measurement points, and in the features extracted to identify the faults, which represent interactions between the bearing faults and the meshing gears, but modified by the casing. These are now well comparable with the experimental results.

Keywords: component mode synthesis, Craig-Bampton, lumped parameter model, gear bearing interaction, fault simulation, localized faults and extended faults.

Introduction

Fault simulation is a valuable and effective tool in understanding the complex interactions between components. Fault simulation allows the analyst to place and dimension the faults, control the operating conditions and gather data from failures without experiencing the cost of actual failures or experimenting with large numbers of seeded faults. Fault simulation facilitates the use of neural networks in the diagnostic/prognostic process as the data required for training the neural network becomes cheaply available.

Lumped parameter models (LPM) are widely utilized to simulate the dynamic behaviour of mechanical systems such as gearboxes. LPMs give reasonable representation of the dynamics of the system if masses can be lumped at certain locations, such as gears, shafts, bearings etc. LPMs have the advantage of simulating the structure using a limited number of degrees-of-freedom (DOF), which facilitates studying the behaviour of gears and bearings in the presence of nonlinearities and geometrical faults [1, 2, 3, 4]. However, it is difficult to account for the casing flexibility in the LPM models, which is an important consideration in lightweight structures such as in aircraft applications and this results in poor spectral matching over a wide frequency range.

7th DSTO International Conference on Health & Usage Monitoring (HUMS 2011)

This paper has been peer reviewed

In the case of continuous systems, where masses are distributed over the structure (gearbox casing), other methods, such as finite element analysis (FEA), are often used to study the behaviour of the structure. The use of FEA results in a large number of DOF, which in turn complicates simulating the whole system's response to the presence of nonlinearities and to gear and bearing faults. This in turn limits the validity of the simulated results and restricts their later usage in the diagnostics and prognostics of the gears and bearings. Hence there is a growing trend to use FE model reduction methods [5] to create accurate low order dynamic models before calculating eigenfrequencies and eigenmodes.

In this paper, a dynamic reduction technique, the so-called, Craig–Bampton reduction technique [6], is utilized to reduce the finite element model of the UNSW gearbox casing. The reduced model is then connected to a lumped parameter model of the internals (shafts, gears and bearings) which has the capacity to simulate faults [3]. The combined model is run in Simulink® environment with localized and extended inner and outer race faults. The response from the combined model at the connecting nodes (bearing centres) and from the modal coordinates is transformed and combined to give the total response at a virtual sensor location, which has been selected to agree with the actual accelerometer position, to compare the results. Thus the total response will not only include the contributions of the dynamics of the internals but also the flexibility and the dynamics of the casing. This makes this approach very attractive as the finite element model has been dramatically reduced from over a hundred thousand degrees of freedom to only 124 DOF.

UNSW Gearbox

The gearbox test rig (Fig.1) under investigation was built by Sweeney [7] to investigate the effect of gear faults on transmission error.

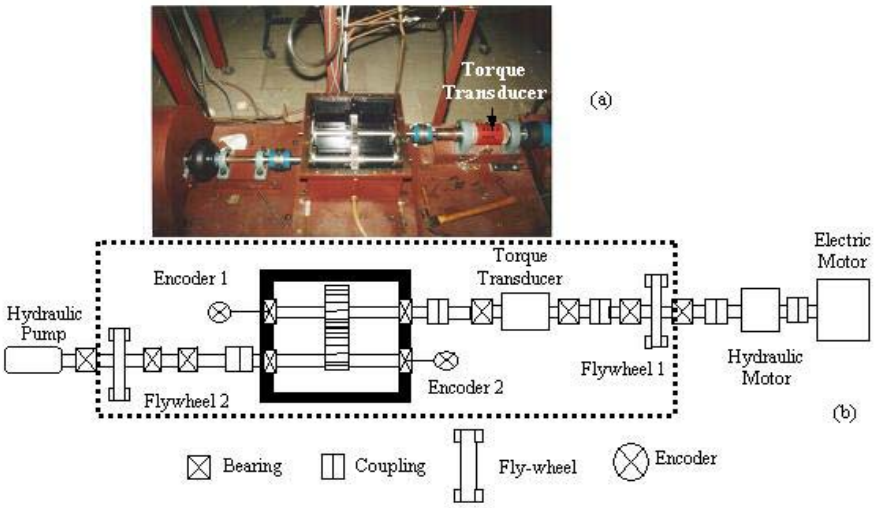


Figure 1 (a) spur gear test rig (b) schematic Diagram of the spur Gearbox Rig (Components of interest contained in dotted box) [7]

In this test rig, the single stage gearbox (in this case a spur gear set with 1:1 ratio and 32 teeth on each gear) is driven primarily by a 3-phase electric motor, but with circulating power via a hydraulic pump/motor set. The input and output shafts of the gearbox are arranged in parallel and each shaft is supported by two double row ball bearings (Koyo 1205). The flywheels are used to reduce the fluctuations of the input and output shaft speeds. The couplings are flexible in torsion and without stiffness in bending, making them very helpful for the attenuation of the shaft torsional vibration

The lumped parameter model (Internals)

Different mathematical models [7, 8,9] have been developed to study the dynamic effects on the transmission error (TE) of the UNSW gearbox. These were lumped parameter models (LPM), which assume that each shaft mass and inertia is lumped at the bearings or at the gears. In all these models, Rolling element bearings (REBs) were modelled as a single degree of freedom (mass-spring) system with constant stiffness. In [3,4] Sawalhi and Randall combined the gear model with a bearing model, which has the capacity to model faults. This resulted in a 34 DOF model (Fig.2) .

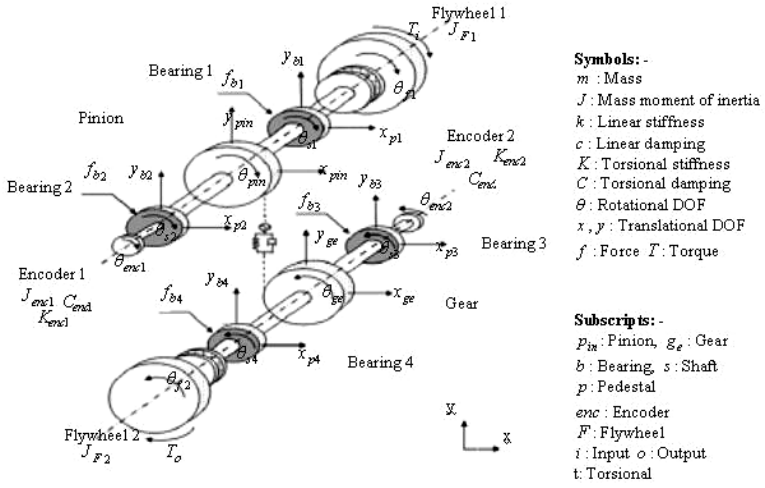


Figure 2 34 DOF Dynamic Model of the gear test rig. (Vertical direction y aligned with the line of action of the gears) [3]

The 34 DOF in the LPM included a 5 DOF bearing model (Fig. 3). The translational degrees of freedom were considered both along the Line of action (LoA) and perpendicular to it. The casing model considered was a simple one and contained only two modal frequencies from hundreds available. This still gave a valid simulation of the gearbox for the purpose of studying its behaviour for a spalled bearing (envelope signal for demodulation of a high frequency resonance) and also in studying the different interactions that exist in the system by comparing simulations with real measurements, for a variety of localized fand extended faults in both gears and bearings [3,4]. It was noticed however that localized faults gave better results than extended faults when compared to the experimental ones.More details about the LPM model and the bearing model can be found in [3].

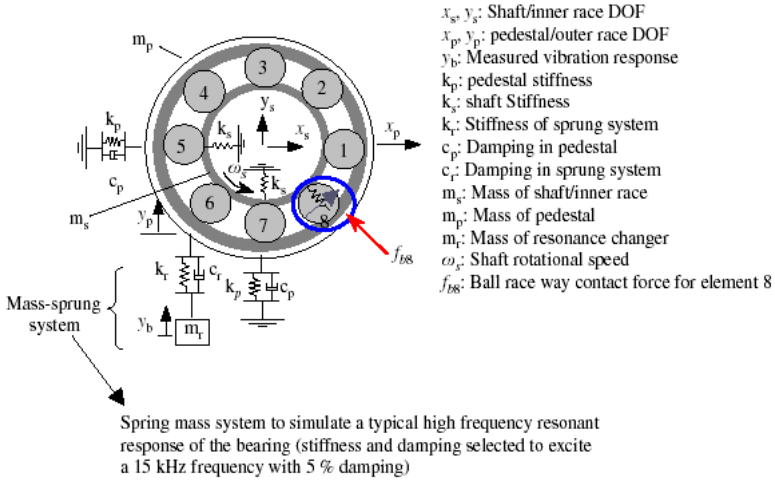


Figure 3 Five degree of freedom bearing-pedestal model [3]

The finite element model (Casing)

The finite element model (FEM) of the casing (104 340 degrees of freedom) is shown in figure 4. The casing is supported by rubber pads, which are simulated here using spring elements at the corners of the casing. It has been updated from an earlier version (shell elements) [10, 11] to the new one which has both solid and shell elements. The model has been compared with experimental modal testing and validated for the lower frequency modes [10]. In the current update the nodes on the hub of each bearing are connected to a centre node using rigid body elements. Thus one centre node is formed at the centre of each bearing, which will eventually capture the flexibility of the casing. This also enables the connecting of this model (a reduced version of it) with the LPM model of the internals - discussed in the previous section - as described in the following sections.

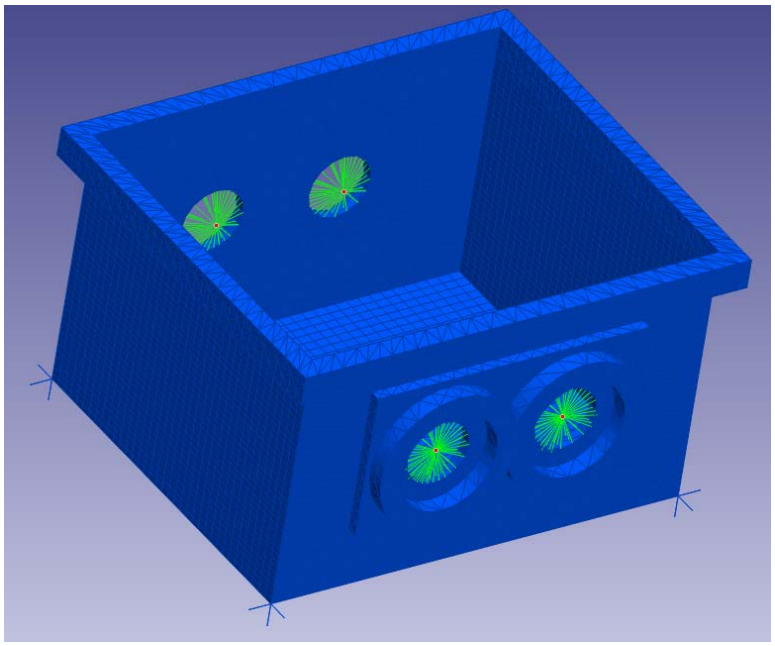


Figure 4 The Finite element model of the UNSW gearbox casing)

FEM reduced model using Craig-Bampton method

Dynamic condensation, as an efficient method for model reduction, was proposed in 1965 [5] by Guyan [12] and Irons [13]. One such method known as the Component Mode Synthesis (CMS) technique [14-16] consists of dividing the complex structure into smaller *substructures* (or *superelements*) and recovering afterwards the dynamic behaviour of the original structure by assembling the *superelements* and considering the equilibrium of nodes at the interfaces between the various components. The dynamic analyses of large structures are often carried out using *superelements* based on the *substructuring* principle.

The static reduction method [12, 13], also known as Irons-Guyan method, produces smaller size system matrices by eliminating the coordinates at which no external force is applied. The reduction method is exact for static problems; however; for dynamic problems large errors may be introduced due to the fact that the DOFs eliminated may experience inertial forces, which cause their dynamic displacements to differ from the static, the deviation increasing with frequency [24]. In such algorithms the reduction takes place by creating master degrees of freedom

The Craig-Bampton method [6] is a dynamic reduction method used to reduce the size of the finite element models. In this method, the motion of the whole structure is represented as a combination of boundary points (so called master degrees of freedom) and modes of the structure assuming the master degrees of freedom are held fixed. Unlike Guyan reduction [12], which only accounts for the stiffness matrix, Craig-Bampton accounts for both the mass and stiffness. Furthermore, it enables defining the frequency range of interest by identifying the modes of interest and including these as a part of the transform matrix. The decomposition of the model into both physical DOFs (master DOFs) and modal coordinates allows the flexibility of connecting the finite elements to other substructures, while maintaining a reasonably good result with a required frequency range. In our application it is very convenient, as the excitation is not from forces, but from geometric mismatch at the connection points (gear transmission error and bearing geometric error). References [17] and [14] were used primarily to give the following summary of the Craig-Bampton method

In the Craig-Bampton reduction method, the equation of motion (dynamic equilibrium) of each superelement (substructure), without considering the effect of damping, can be expressed as in Eqn. (1):

$$[M]\{\ddot{u}\}+[k]\{u\}=\{F\} \tag{1}$$

where $[M]$ is the mass matrix, $[k]$ is the stiffness matrix, $\{F\}$ is the nodal forces, $\{u\}$ and $\{\ddot{u}\}$ are the nodal displacements and accelerations respectively.
The key to reducing the substructure is to split the degrees of freedom into master $\{u_m\}$ (at the connecting nodes) and slaves $\{u_s\}$ (at the internal nodes). The mass, the stiffness and the force matrices are re-arranged accordingly as follows:

$$\overbrace{\begin{bmatrix} M_{mm} & M_{ms} \\ M_{sm} & M_{ss} \end{bmatrix}}^{M}\begin{Bmatrix} \ddot{u}_m \\ \ddot{u}_s \end{Bmatrix}+\overbrace{\begin{bmatrix} k_{mm} & k_{ms} \\ k_{sm} & k_{ss} \end{bmatrix}}^{k}\begin{Bmatrix} u_m \\ u_s \end{Bmatrix}=\begin{Bmatrix} F_m \\ 0 \end{Bmatrix} \tag{2}$$

The subscript *m* denotes master, *s* denotes slave. Furthermore, the slave degrees of freedom (internals) can be written using generalized coordinates (modal coordinates (q) using the fixed interface method, i.e. using the mode shapes of the superelement by fixing the master degrees of freedom nodes (connecting/ boundary nodes). The transformation matrix (T) is the one that achieves the following:

$$\begin{Bmatrix} u_m \\ u_s \end{Bmatrix}=T\begin{Bmatrix} u_m \\ q \end{Bmatrix} \tag{3}$$

For the fixed interface method, the transformation matrix (T) can be expressed as shown in Eqn (4):

$$T=\begin{bmatrix} I & 0 \\ G_{sm} & \phi_s \end{bmatrix} \tag{4}$$

where,

$$G_{sm}=-k_{ss}^{-1}k_{sm} \tag{5}$$

and ϕ_s is the modal matrix of the internal DOF with the interfaces fixed.

Applying this transformation, the number of DOF of the component will be reduced. The new reduced mass and stiffness matrices can be extracted using Eqns (6) and (7) respectively:

$$M_{reduced}=T^tMT \tag{6}$$

and

$$k_{reduced}=T^tkT \tag{7}$$

Thus Eqn (2) can be re-written in the new reduced form using the reduced mass and stiffness matrices as well as the modal coordinates as follows:

$$\overbrace{\begin{bmatrix} M_{bb} & M_{bq} \\ M_{qb} & M_{qq} \end{bmatrix}}^{M_{reduced}}\begin{Bmatrix} \ddot{u}_m \\ \ddot{q} \end{Bmatrix}+\overbrace{\begin{bmatrix} k_{bb} & 0 \\ 0 & k_{qq} \end{bmatrix}}^{k_{reduced}}\begin{Bmatrix} u_m \\ q \end{Bmatrix}=\overbrace{\begin{Bmatrix} F_m \\ 0 \end{Bmatrix}}^{F_{reduced}} \tag{8}$$

where M_{bb} is the boundary mass matrix i.e. total mass properties translated to the boundary points.

k_{bb} is the Interface stiffness matrix i.e. stiffness associated with displacing one boundary DOF while the others are held fixed

M_{bq} is the component matrix (M_{qb} is the transpose of M_{bq})

If the mode shapes have been mass normalized (typically they are) then:

$$k_{qq} = \begin{bmatrix} \backslash & & 0 \\ & \lambda_i & \\ 0 & & \backslash \end{bmatrix} \tag{9}$$

where λ_i is the eignvalues; $\lambda_i = k_i / m_i = \omega^2{}_i$

and,

$$M_{qq} = \begin{bmatrix} \backslash & & 0 \\ & I & \\ 0 & & \backslash \end{bmatrix} \tag{10}$$

Finally the dynamic equation of motion (including damping) using the Craig - Bampton transform can be written as:

$$\begin{bmatrix} M_{bb} & M_{bq} \\ M_{qb} & I \end{bmatrix} \begin{Bmatrix} \ddot{u}_m \\ \ddot{q} \end{Bmatrix} + \begin{bmatrix} 0 & 0 \\ 0 & 2\zeta\omega \end{bmatrix} \begin{Bmatrix} \dot{u}_m \\ \dot{q} \end{Bmatrix} + \begin{bmatrix} k_{bb} & 0 \\ 0 & \omega^2 \end{bmatrix} \begin{Bmatrix} u_m \\ q \end{Bmatrix} = \begin{Bmatrix} F_m \\ 0 \end{Bmatrix} \tag{11}$$

where $2\zeta\omega$ = modal damping (ζ = fraction of critical damping)

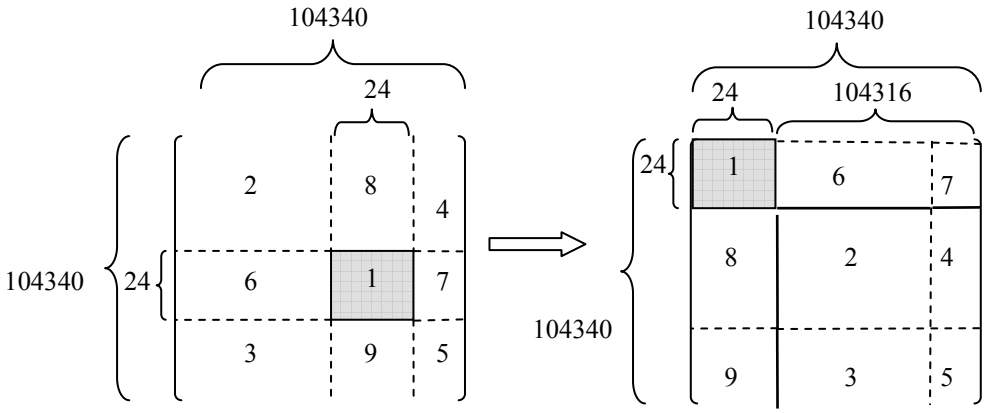
Craig-Bampton reduction in Matlab®

The finite element model of the UNSW gearbox shown in Fig. 4 has 104 340 DOFs. Thus the mass matrix [*M*] and the stiffness matrix [*k*] are square matrices of size 104 340×104 340. There are 4 boundary DOFs (nodes to be connected with the LPM system). With 6 DOF at each node there are 24 master degrees of freedom (boundary DOFs). If we are to retain the first 100 modes (modes up to 4 kHz), then the reduced model will have mass and stiffness matrices [$M_{reduced}$] and [$k_{reduced}$] of size 124×124 i.e. 24 boundary coordinates and 100 modes

The process of obtaining the reduced mass and stiffness matrices has been done on a step-by-step basis using FEMtools® and Matlab® as follows:

(1) The mass matrix [*M*] and stiffness matrix [*k*] (both in binary format) were extracted from the finite element package (FEMtools® used in this study) and imported into Matlab® as *sparse* matrices: the size of the matrix is (104 340×104 340). Note that without using the sparse matrix, it is practically impossible to work with such a size of matrix in Matlab®.

(2) [*M*] and [*k*] were rearranged to have the master degrees of freedom (24×24) in the upper left hand corner of the matrix, the slaves (104 316×104 316) in the lower right hand corner. Fig. 5 illustrates the re-arrangement applied to both the mass and the stiffness matrices.



Matrix 1: Master degrees of freedom [M_{mm} for mass and k_{mm} for stiffness]
Matrices 6, 7: component matrix [M_{ms} for mass and k_{ms} for stiffness]
Matrices 8, 9 : inverse [M_{ms} for mass and k_{ms} for stiffness]
Matrices 2, 4, 3, 5: Slave degrees of freedom [M_{ss} for mass and k_{ss} for stiffness]

Figure 5 Rearranging the extracted mass and stiffness matrices

This rearrangement (Fig. 6) gives an order equivalent to the one shown in Eqn. 2.

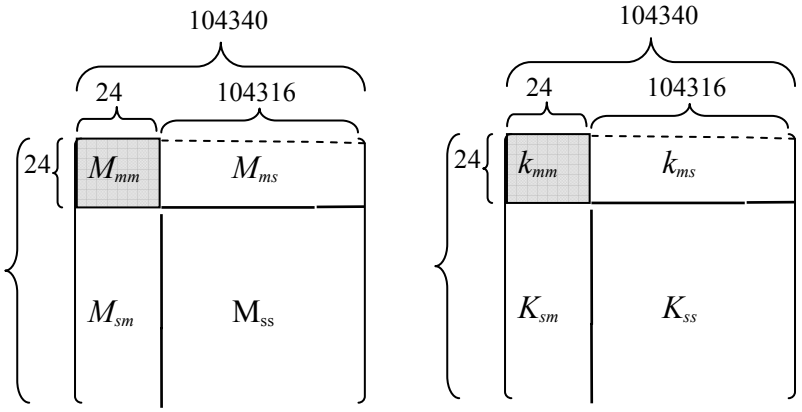


Figure 6 Rearranged mass and stiffness matrices

(3) After rearranging the mass and stiffness matrices as shown in Fig.6, the G_{sm} matrix (Eqn. 5) was calculated. Note that the backslash operator (\) was used instead of the inverse process. The size of G_{sm} is 104 316×24.

(4) The ϕ_s matrix (mode shapes of the gearbox with fixed master degrees of freedom) was extracted from FEMtools®. Each mode shape was placed in a vector, thus the

size of ϕ_s is $104\,316 \times 100$ (Slave degrees of freedom$\times$ the number of retained modes)

(5) The T matrix was formed using Eqn. 4.

(6) The reduced mass and stiffness matrices (124 × 124) were found using Eqns.6 and 7 respectively. However, the off-diagonal zeros as observed in Eqns.9, 10 and 11 have to be enforced as the direct calculations resulted in values of order 10^{-8} to 10^{-16} (practically zeros). Keeping these values affects the stability of the solution and in particular gives a near singular inverse mass matrix.

The combined (LPM- reduced FEM) model

The reduced mass and stiffness matrices ($[M_{reduced}]$ and $[k_{reduced}]$) were combined with the LPM model in the Simulink® environment. The combination was achieved by re-writing the equations of motion at the connecting nodes. The LPM model of the internals has 22 DOFs (12 DOFs previously introduced to model the casing (4DOFs at each bearing)). The total DOFs for the new combined model is 146. 46 of these are physical degrees of freedom while 100 are modal coordinates. The modal damping (Eqn. 10) was introduced at this stage (ζ = 4%). The model was then solved and the acceleration responses were obtained. Eqn. 3 was used to expand both the physical and the modal responses back to the slave degrees of freedom. This gives a combination of both the physical response from the master degrees of freedom and the modal coordinates, which can be achieved by combining Eqns. 3 and 4 as follows:

$$\begin{Bmatrix} u_m \\ u_s \end{Bmatrix} = \begin{bmatrix} I & 0 \\ G_{sm} & \phi_s \end{bmatrix} \begin{Bmatrix} u_m \\ q \end{Bmatrix} \tag{12}$$

The responses at the slave degrees of freedom can be obtained using equation (13) as follows:

$$u_s = G_{sm} u_m + \phi_s q \tag{13}$$

This translates back to any slave degree of freedom of an interest.

Results and Discussions

The improvements gained from the combined LPM-Condensed FEM are demonstrated on the case of an extended inner race fault (15 mm). It has been shown earlier [4] that in the case of localized faults, the LPM model gave reasonable results and the comparisons between the experimental and simulated results were considered good, especially when performing envelope analysis (demodulation of a high frequency resonance). The interaction between the gears and the bearings in the case of localized faults is additive, meaning that the bearing fault excites high frequency bands away from the gear dominance bands (low frequency region). This enables filtering and separating the fault signal from the gear signal. In the case of extended

faults, the interactions have been shown to be multiplicative; i.e. the extended fault cannot be separated by a simple high pass filtration as it modulates the gear signal. The process to affirm the presence of such a fault is through using spectral correlation functions (SCF) [18]. Spectral correlation has the property that it isolates the spectral content coming from sources at each cyclic (modulating) frequency, whether the carrier component is deterministic or random. If deterministic components are removed at the outset (which would eliminate gear signals) only the random (second order cyclostationary) components remain and these most likely come from extended bearing fault signals [18]. The normal power spectrum is found at zero cyclic frequency. Thus, spectrum comparisons are made (at a cyclic frequency equal to shaft speed) between the good and the faulty signals after removal of the periodic/deterministic parts, using time synchronous averaging (TSA), self adaptive noise cancellation (SANC) or discrete/Random separation (DRS) [19, 20]. If large dB differences are seen in the low frequency region (as well as at high frequencies, subject to the roughness of the faults) then the fault is confirmed to be an extended inner race rather than a gear fault.

Fig. 7 shows the normal power spectral density comparisons for the raw experimental signal (7.a), the LPM result (7.b) and the combined model (7.c). The variations from the LPM are quite noticeable in the low frequency region (more natural frequencies added up to 4 kHz). This has now a better resemblance to the experimental measured signals. An increase in the dB difference (4-6 dB) as a result of the faults is seen in the high frequency region, but a diagnosis cannot be made at this stage; as this may be the result of an increase in the stationary noise.

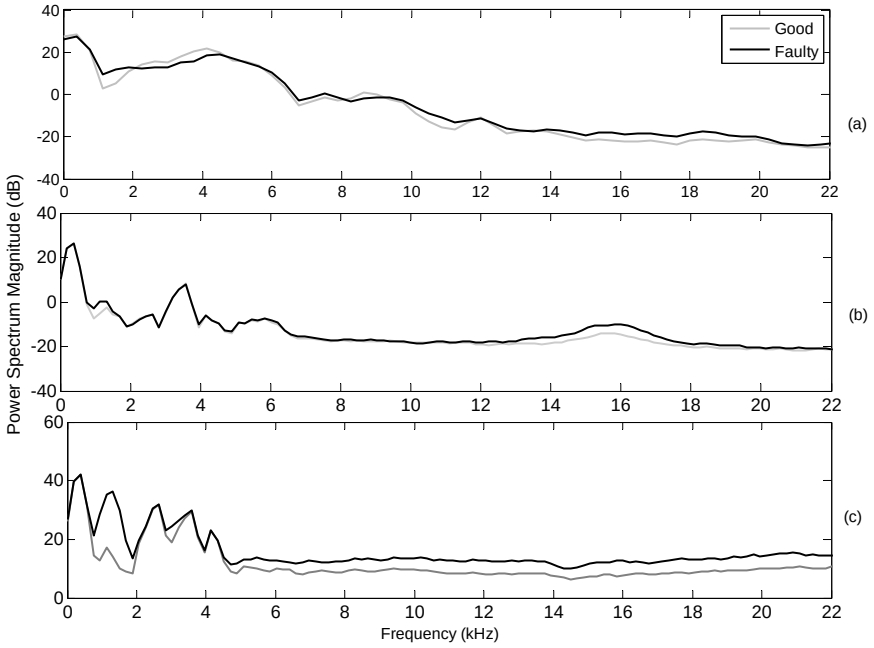


Figure 7 Comparisons of broadband spectra for the extended inner race fault (a) Experimental (b) LPM model (c) Condensed model

The 3D plots of the SCF for the experimental results, the condensed model and the LPM are shown in Figs 8, 9 and 10 respectively. The resemblance is much closer between the experimental results and the condensed model, than those of the LPM

model. A continuous spectrum (along the frequency axis) indicates a cyclic event. This is clearly seen at the cyclic frequency of the shaft speed (10 Hz). It is noticed also that the second and the third harmonics of the shaft speed as well as the BPFI (ballpass frequency, inner race) at 71.2 Hz are also present over a wide frequency range. BPFI is not seen as clearly in the LPM result.

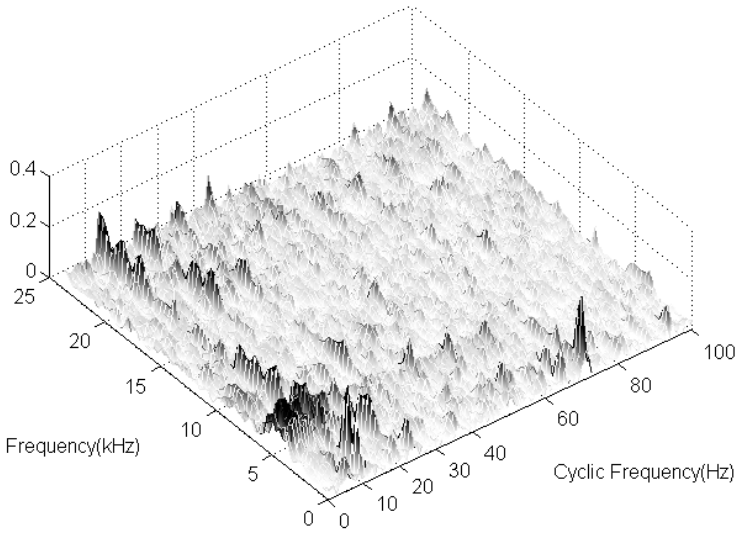


Figure 8 Spectral correlation function (SCF) for the extended inner race fault (Experimental result) [3]

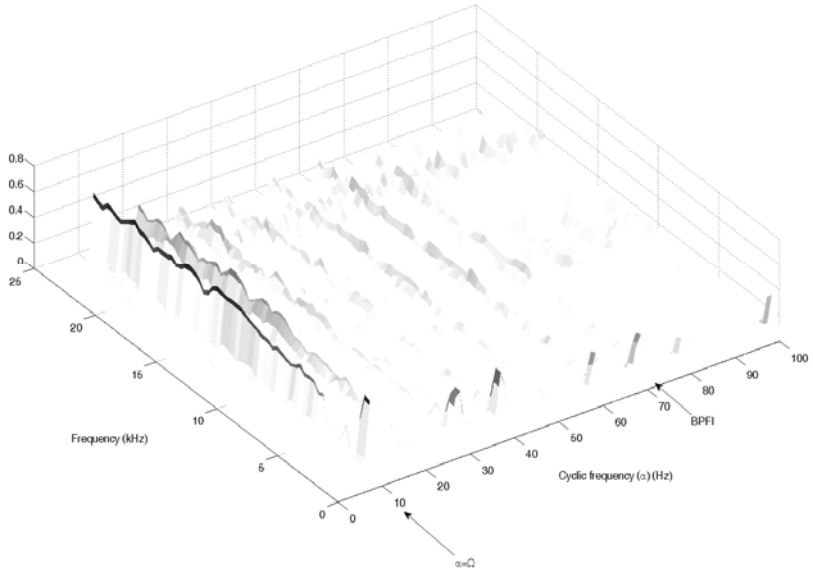


Figure 9 Spectral correlation function (SCF) for the extended inner race fault (Condensed model)

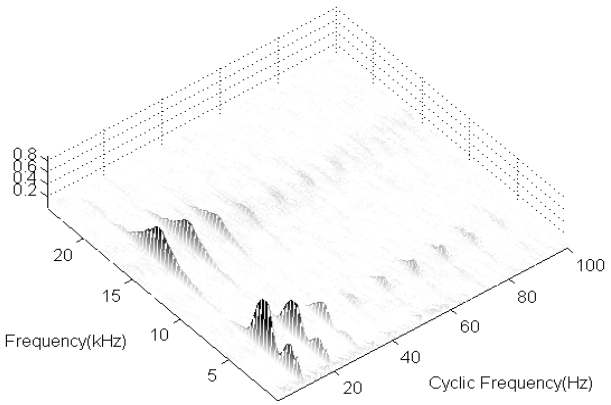


Figure 10 Spectral correlation function (SCF) for the extended inner race fault (LPM simulated result) [3]

Fig.11 presents the SCF comparisons for the residuals (periodic parts removed using DRS) at the cyclic frequencies: $\alpha = 0$ and $\alpha = \Omega$ (shaft speed, 10 Hz in this study) for the experimental results and the simulated ones (condensed model). Although the results are presented up to 20 kHz, the validity of these in the simulated ones is up to 4 kHz, as no modes above that were considered in the model.

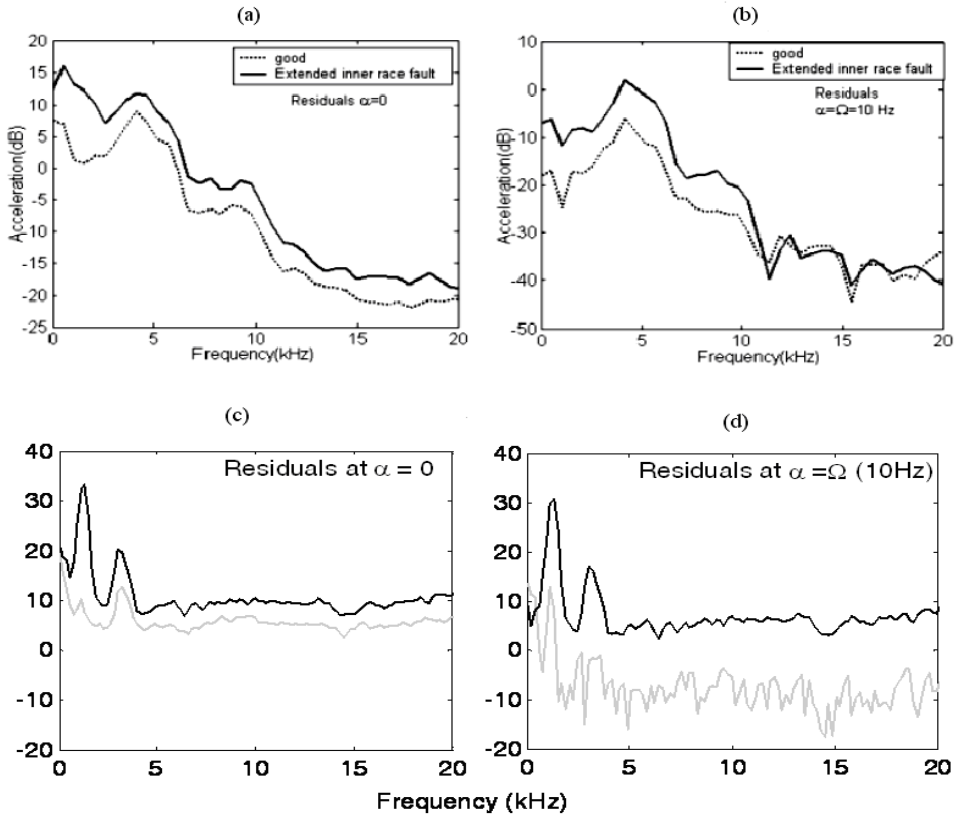


Figure 9 Cyclic spectrum comparisons. Top: measured. Bottom: simulated. (a) measured residuals compared at $\alpha = 0$ (b) measured residuals compared at $\alpha = \Omega$ (c) simulated residuals compared at $\alpha = 0$ (d) simulated residuals compared at

For $\alpha = 0$, the power spectrum level for the faulty bearing is higher than that of the good bearing for both simulated and measured signals. The increase in the dB difference spreads across the whole frequency range and there are no distinct frequency bands, where the increase is greater. As the comparison is made at $\alpha = 0$, no conclusion could be drawn as to the source of excitation, as this increase in the dB difference could be the result of an increase in the stationary noise, which is still present at $\alpha = 0$. For $\alpha = \Omega$ it is noticed that the highest increase in the dB difference appears mainly in the low frequency region (where the fault modulates the gearmesh frequencies). The increase in the dB difference at $\alpha = \Omega$ implies the existence of an extended fault in the inner race (as no gear component or stationary noise are present in this comparison). In the measured signal, the increase is noticed mainly in the low frequency region, as the fault has a smooth exit, so that the higher frequency region was not excited. A smoother exit will be simulated in future work.

Conclusions

The application of the Craig-Bampton finite element model reduction technique for the simulation of dynamic behaviour of a complex machine structure, such as a gearbox, is described. The reduced mass and stiffness matrices obtained through the dynamic reduction of the casing were incorporated into the lumped parameter model of the gearbox. The results of simulating an extended inner race bearing fault in the new model were compared to the experimental measurements and the results of the lumped parameter model only. Improvements are reported in the low frequency region. The cyclic spectrum comparison after removing the contribution of gears shows an increase in the dB difference at the relevant cyclic frequencies for the combined model (LPM and reduced FEA) and shows the presence of the extended inner race fault more clearly than before.

Acknowledgments

This work is supported by the Australian Defence Science and Technology Organization (DSTO) as a part of their Centre of Expertise scheme

References

[1] J. Sopanen, A. Mikkola, Dynamic model of a deep-groove ball bearing including localized and distributed defects. Part 1: Theory, in: Proceedings of the Institution of Mechanical Engineers, vol. 217, Part K: J. Multi-body Dynamics, 2003, pp. 201–211.

[2] M. Tiwari, K. Gupta, O. Prakash, Dynamic response of an unbalanced rotor supported on ball bearings, Journal of Sound and Vibration 238 (2000) 757–779.

[3] N. Sawalhi and R. B. Randall, "Simulating gear and bearing interactions in the presence of faults: Part II: Simulation of the vibrations produced by extended bearing faults," *Mechanical Systems and Signal Processing,* vol. 22, pp. 1952-1966, 2008.

[4] N. Sawalhi and R. B. Randall, "Simulating gear and bearing interactions in the presence of faults: Part I. The combined gear bearing dynamic model and the simulation of localised bearing faults," *Mechanical Systems and Signal Processing,* vol. 22, pp. 1924-1951, 2008.

[5] Z.-Q. Qu, *Model Order Reduction Techniques :with Applications in Finite Element Analysis* Springer, 2004.

[6] R. Craig and M. Bampton, Coupling of substructures for dynamic analysis. *Amer. Inst. Aero. Astro. J.* **6** 7 (1968), pp. 1313–1319.

[7] P. Sweeney, "Transmission error measurement and analysis " Ph. D. Dissertation, Mechanical & Manufacturing Engineering, Faculty of Engineering, University of New South Wales, Sydney, Australia, 1994.

[8] S. Du, "Dynamic modelling and simulation of gear transmission error for gearbox vibration analysis," Ph.D. Dissertation, Mechanical & Manufacturing Engineering, Faculty of Engineering, University of New South Wales, Sydney, Australia, 1997.

[9] H. Endo, "Simulation of gear faults and its application to the development of differential diagnostic technique " Ph. D. Dissertation, Mechanical & Manufacturing Engineering, Faculty of Engineering, University of New South Wales, Sydney, Australia, 2005.

[10] N. Sawalhi and R. B. Randall, "Improved Simulation of Faults in Rolling Element Bearings in Gearboxes," presented at the 9th International Conference on Vibrations in Rotating Machinery, 8-10 September, UK, 2008.

[11] N. Sawalhi and R. B. Randall, "A Combined Lumped Parameter and Finite Element Model of a Single Stage Gearbox for Bearing Fault Simulation," presented at the COMADEM 2008 (Condition Monitoring and Diagnostic Engineering Management), Prague, Czech Republic, 2008.

[12] B.M. Irons (1965), Structural eignvalue problems-elimination of unwanted variables. AIAA journal, 3(5):961-962

[13] R.J. Guyan (1965), Reduction of stiffness and mass matrices. AIAA Journal, 30(3)772-780.

[14] C. Carmignani, P. Forte, and G. Melani, "Component modal synthesis modeling of a gearbox for vibration monitoring simulation," presented at the The Sixth International Conference on Condition Monitoring and Machinery Failure Prevention Technologies, Dublin, Ireland, 2009.

[15] S. Ulf, "COMPONENT MODE SYNTHESIS - A method for efficient dynamic simulation of complex technical systems," Technical Report, Department of Machine Design, The Royal Institute of Technology (KTH), S-100 44 Stockholm, Sweden2003.

[16] H. N. Bayoumi, "Interfacing FEA and Multibody Simulation Through Component Mode Synthesis," in *ASME Conference Proceedings*, 2005, pp. 1387-1392.

[17] S. Gordan, FEMCI the book: http://femci.gsfc.nasa.gov/craig_bampton/index.html

[18] J. Antoni, and R.B. Randall, Differential diagnosis of gear and bearing faults, Journal of Vibration and Acoustics, vol.124, pp. 165-171(2002).

[19] J. Antoni and R. B. Randall, "Unsupervised noise cancellation for vibration signals: part I--evaluation of adaptive algorithms," *Mechanical Systems and Signal Processing,* vol. 18, pp. 89-101, 2004.

[20] J. Antoni and R. B. Randall, "Unsupervised noise cancellation for vibration signals: part II--a novel frequency-domain algorithm," *Mechanical Systems and Signal Processing,* vol. 18, pp. 103-117, 2004.